Extrinsic origin of ferromagnetism in doped ZnO

Javier Blasco,* Fernando Bartolomé, Luis M. García and Joaquín García

Received 3rd January 2006, Accepted 30th March 2006
First published as an Advance Article on the web 21st April 2006
DOI: 10.1039/b518418e

Different synthetic routes have been tested to prepare bulk doped ZnO. The doping elements were Mn, Fe and Co. We were able to prepare single-phase compounds at high temperature by using ceramic procedures and at very low temperature using a sol–gel method. No ferromagnetism has been observed for these samples. In contrast, spontaneous magnetization is observed in samples obtained from non-optimal conditions and exhibiting secondary phases. Magnetic impurities have been easily identified for Fe- and Co-doped samples. However, the nature of the room temperature magnetic impurity for the Mn-based compound is not so clear and different possibilities are discussed. We have also checked the effect of the grain size on the magnetic properties by synthesizing nano-materials using a sol–gel route. The single-phase nano-compounds are also not ferromagnets showing similar properties to the well-sintered polycrystalline materials.

1. Introduction

The transparent conducting oxides are basic materials for remarkable applications in various fields of optical and electronic devices. Recent theoretical studies[1] claiming a ferromagnetic ground state in substituted ZnO have opened new expectations for these materials such as the magnetic control of the optical and electrical properties.[2,3] The finding of room temperature ferromagnetism in some deposited thin films seemed to verify previous theoretical predictions[4–7] though several studies have thrown doubts on the intrinsic nature of the magnetic behaviour.[8–10] Recently, this controversy has been extended to ceramic bulk materials due to the finding of ferromagnetism in $Zn_{1-x}Mn_xO$ or $Zn_{1-x}Co(Cu)_xO$ polycrystalline materials.[11,12] These authors claimed the preparation of homogeneous and ferromagnetic single phases using very low sintering temperatures. In parallel, room temperature ferromagnetism was also achieved by mechanical alloying of ZnO and MnO_2 powders.[13] In both studies, the use of further sintering procedures at higher temperature seemed to be detrimental for the ferromagnetism.

Nevertheless, other researchers have shown that the synthetic route described in ref. 11 leads to multi-phase materials. Single phases can only be obtained by sintering at higher temperatures and they are not magnets at room temperature.[14,15]

The aim of the present work is to shed light on this controversy. In order to do this, we have synthesized $Zn_{0.96}M_{0.04}O$ samples (M being Fe, Co or Mn) following different synthetic routes. There are several reasons for the choice of these compounds. On the one hand, Mn-, Co- and Fe-doping are candidates to show ferromagnetic ground states.[1,16] On the other, the doping level of 4% is close to the optimum value predicted in ref. 16. Finally, it would be difficult to find small impurities using smaller amounts of doping agent.

Our synthetic procedures cover a wide range of synthesis conditions. In order to test the effects of the grain size on the magnetic properties, we have also prepared nano-materials by means of a sol–gel method using very low temperature. Therefore, these compounds can be compared to the ones obtained by mechanical alloying.[13] Our results strongly suggest that ferromagnetism is only due to the presence of magnetic impurities whereas single phases behave as paramagnetic semiconductors.

2. Experimental

All samples were characterized by means of X-ray diffraction by using a D-MaxB Rigaku system. We used Cu K_α radiation and the patterns were collected from 15° up to 100° in steps of 0.03°. Different counting times were used depending on each sample. Structural refinements were carried out for single phases by using the Rietveld method and the Fullprof program.[17]

Magnetization measurements were carried out by using a Superconducting Quantum Interference Device (SQUID) magnetometer working up to 5 T and down to 5 K.

Several sets of $Zn_{0.96}M_{0.04}O$ samples were prepared as described in the following routes.

a) Ceramic procedure at low temperature

Stoichiometric amounts of ZnO and $MnCO_3$ (Fe_2O_3 or Co_3O_4) were mixed, ground and calcined at 400 °C for 8 h in air. The resulting powders were ground and pressed into pellets. They were sintered at 500 °C for 12 h in the same atmosphere. The Fe- and Co-based pellets were grey while the Mn-based one was orange–brown.

The aim of this procedure was to reproduce the results of ref. 11 that claim the synthesis of ferromagnetic single-phase samples. It is noteworthy that we used $MnCO_3$ instead of MnO_2 as the Mn source.

Instituto de Ciencia de Materiales de Aragón, CSIC-Universidad de Zaragoza, Departamento de Física de la Materia Condensada, Pedro Cerbuna 12, 50009, Zaragoza, Spain. E-mail: jbc@unizar.es; Fax: +34-976-761219; Tel: +34-976-762419

b) Ceramic procedure at low oxygen pressure

As described in procedure a, stoichiometric amounts of ZnO and $MnCO_3$ (Fe_2O_3 or Co_3O_4) were mixed, ground and calcined at 400 °C for 8 h in air. Then, the powders were ground, pressed into pellets and placed in a Morris-Research furnace able to work up to 200 bars of pressure. Mo powder was also added in another crucible as oxygen getter. The tube was filled with Ar at two selected pressures (2 or 175 bars) and the pellets were sintered at two selected temperatures (600° or 850 °C). The choice of Mo was due to its oxidation reactions: $Mo + O_2 \leftrightarrows MoO_2 + \frac{1}{2} O_2 \leftrightarrows MoO_3$. The resulting Mo powder was analyzed by X-ray diffraction revealing a mixture of Mo and MoO_2 in all cases. The lack of MoO_3 guarantees a low oxygen partial pressure (pO_2). pO_2 would be less than $10^{-12.5}$ and $10^{-8.5}$ bar at 600 °C and at 850 °C, respectively.[18]

The aim of this route is to approach the experimental conditions in pO_2 for thin film deposition using high-vacuum chambers. The pellets sintered at 600 °C showed grey and colored regions indicating the lack of homogeneity. The pellets sintered at 850 °C were bottle-green, olivine-green and orange for Co-, Fe- and Mn-based compounds, respectively.

c) Conventional ceramic procedure in inert atmosphere

The calcination process was like that described in procedure b. The resulting powders were ground, pressed into pellets and sintered in a current flow of Ar for 12 h. Two selected temperatures were used for the sintering step, 920° and 1150 °C.

The purpose of this procedure was to complete the previous route using an inert atmosphere with moderately low pO_2 ($\sim 10^{-3}$–10^{-4}).

The pellets showed similar colors to those of procedure b, though some black points were clearly visible in the Fe-based pellet.

d) Sol–gel method

Stoichiometric amounts of ZnO and $MnCO_3$, Fe or $(CH_3COO)_2Co{\cdot}4H_2O$, were dissolved in nitric acid solution. Then, citric acid and ethylene glycol were added (4 g and 2 ml per g of precursor, respectively) and light-yellow, pink and bright-yellow solutions were obtained for Mn-, Co- and Fe-based solutions. They were heated up to gel formation. The gel was fired at 210 °C overnight. The resulting brown resin was calcined in different flowing atmospheres, oxygen, air and Ar. Different processes were used depending on each sample and the grain size desired (see Results section).

The aim of this route was to prepare single phases composed of fine particles in order to account for the effects of grain size in the magnetic properties of these compounds. Another purpose was to establish the appropriate comparisons to the samples obtained from mechanical alloying.[13]

3. Results

3.1. Samples prepared from ceramic method at low temperature

The samples prepared following this synthetic route are not single phase. This is clearly seen in the patterns collected in Fig. 1. All of these patterns show the presence of the hexagonal ZnO as main phase. The refined lattice parameters were a = 3.2488(2) Å and c = 5.2036 (2) Å for the three samples indicating that this thermal treatment is not enough to provoke the diffusion of the metal (Mn, Fe or Co) into the ZnO phase, in agreement with previous results.[14]

Different secondary phases are present in these compounds. The X-ray pattern of the Co-based sample reveals the presence of the starting material, Co_3O_4. Fe_2O_3 and tiny amounts of a spinel phase (similar to Fe_3O_4) are identified for the Fe-based sample. The Mn-based sample does not show traces of Mn precursor such as $MnCO_3$, Mn_2O_3, MnO or MnO_2. The pattern reveals instead the presence of a secondary phase with broad peaks that can be indexed in a cubic cell with a =8.362 Å. This cell concurs with the one described for the cubic $ZnMnO_3$ reported in a pioneering work.[19] This impurity has also been observed in $Zn_{1-x}Mn_xO$ samples annealed in high oxygen pressure.[20] However, the synthesis of $ZnMnO_3$ needs strong oxidative conditions and it has the rhombohedral ilmenite lattice.[21] Moreover, a detailed inspection of the X-ray data of ref. 19 makes evident the presence of a F-centered lattice with allowed reflections compatible with a cubic spinel. In order to check this point, we have studied the possible existence of cubic spinels $Zn(Mn_{2-x}Zn_x)O_4$. We were successful in preparing metastable Zn-rich spinels showing a cubic cell and a mixed Mn valence at the octahedral site. Some phases can only be prepared at very low temperature and decompose into ZnO and $ZnMn_2O_4$ upon heating. For instance, Fig. 2 shows the pattern for $Zn_{1.7}Mn_{1.3}O_4$ prepared by the sol–gel method (see also section 3.4). It shows a cubic spinel cell without the presence of secondary phases.

Isothermal magnetization measurements at 5 K are shown for the three samples in Fig. 3. The Co-based sample shows positive linear behavior (paramagnetic-like) that can be understood in terms of the two magnetic contributions expected.

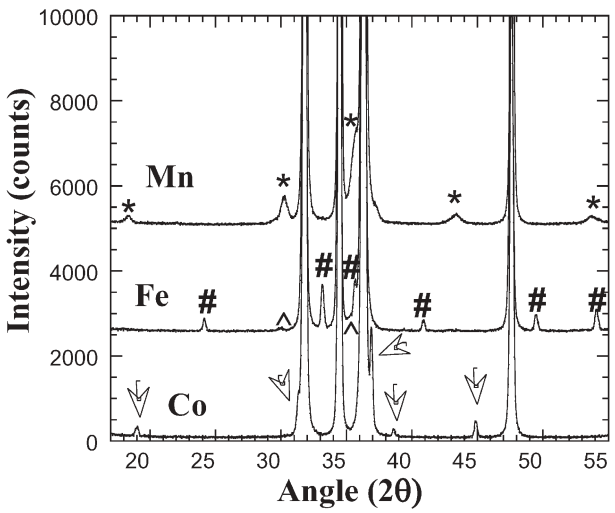

Fig. 1 Detail of the X-ray patterns for the Mn-, Fe- and Co-doped samples synthesized following the solid state procedure at low temperature. Arrows, #, ⋀ and * indicate the peak positions for Co_3O_4, Fe_2O_3, $Fe_{3-x}Zn_xO_4$ and $ZnMnO_3$ phases, respectively. The Mn and Fe patterns have been shifted upwards (2500 and 5000 counts, respectively) for the sake of clarity.

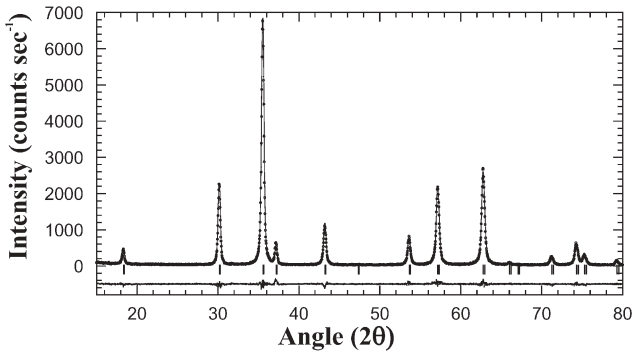

Fig. 2 Rietveld plots for the $Zn_{1.7}Mn_{1.3}O_4$ phase prepared by the sol–gel method and sintered at 600 °C for 15 h. The symbols have the usual meanings. We have used the $Fd\bar{3}m$ space group and the lattice parameter was a = 8.3640(6) Å. Reliability factors are very good. For instance, χ^2 =1.4 and R_{Bragg} =1.7 according to definitions from ref. 17.

ZnO is diamagnetic with a value[14] of -0.33×10^{-6} emu g^{-1} and Co_3O_4 orders[22] antiferromagnetically at $\sim$40 K.

The Fe-based sample has a clear spontaneous magnetization at 5 K although it behaves as paramagnet at room temperature (not shown here). The ferromagnetic contribution at 5 K has been estimated to be $\sim 4.7 \times 10^{-4}$ μ_B fu^{-1} and it can be ascribed to the tiny amounts of the spinel phase and since its Curie temperature (T_C) is below room temperature, a partial incorporation of Zn into the Fe_3O_4, *i.e.* $Fe_{3-x}Zn_xO_4$ composition, can be inferred.

The most surprising results correspond to the Mn-based sample. This compound shows a strong paramagnetic contribution and spontaneous magnetization also at room temperature as can be seen in the inset of Fig. 3, in agreement with previous reports.[11,23] This fact indicates that room temperature ferromagnetism can be obtained using Mn precursors different from MnO_2. However, $MnCO_3$ seems to be more appropriate than MnO to form the ferromagnetic phase[23] probably due to the higher reactivity of the MnO produced after $MnCO_3$ decomposition. The calculated net magnetic moment at room temperature is $\sim 1.4 \times 10^{-3}$ μ_B Mn^{-1} indicating a tiny amount of magnetic phase and even the secondary phase seems to be mainly paramagnetic.

3.2. Samples prepared at low oxygen pressure

Fig. 4 shows the patterns of the samples sintered at 600 °C and at 175 bars of Ar pressure in a low pO_2 ($\sim 10^{-12.5}$). All samples show the same main phase, ZnO, with identical lattice parameters and similar to those obtained in section 3.1. This result indicates that ZnO is not altered significantly in these conditions. Changes are observed in the secondary phases. The Mn-based sample has two additional phases, $ZnMn_2O_4$ and tiny amounts of MnO. We also observe another two phases, Co_3O_4 and CoO, for the Co-based sample. The Fe-based sample instead only showed a secondary phase: magnetite. Therefore, the use of Mo as oxygen getter leads to a reduction of the doping sources but does not affect the zinc oxide. There are no noticeable changes by modifying the external pressure at this temperature, and similar results were achieved at 2 bars of external pressure.

The magnetic properties reflect the chemical compositions of these samples as can be seen in Fig. 5. In this way, the Co-based sample is paramagnetic down to 5 K in agreement with the presence of CoO and Co_3O_4. The Mn-based sample is paramagnetic at room temperature but it shows a ferromagnetic component at 5 K that can be ascribed to the presence of $ZnMn_2O_4$ whose T_C is close to 40 K.[24] The Fe-based sample shows a strong spontaneous magnetization up to room temperature due to the presence of magnetite.

The increase of sintering temperature leads to significant changes in the phase compositions of the samples. Single phases can be prepared for Mn- and Fe-based compounds by sintering at 850 °C at low pO_2. For instance, Fig. 6 shows the Rietveld plot for $Zn_{0.96}Mn_{0.04}O$ prepared at 175 bars of total

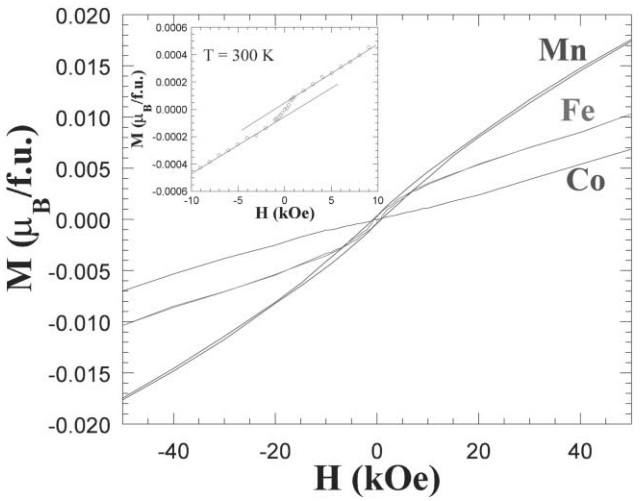

Fig. 3 Magnetization loops for Mn-, Fe- and Co-doped samples of Fig. 1 at 5 K. The data for Fe and Co samples have been multiplied by four for the sake of comparison. Inset: magnetization loop for the Mn-based sample at 300 K. The straight lines show the linear behavior of the paramagnetic contribution.

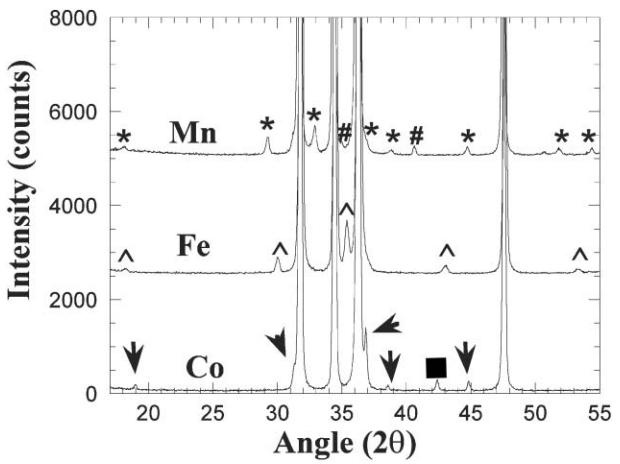

Fig. 4 Detail of the X-ray patterns for the Mn-, Fe- and Co-doped samples synthesized at 600 °C in a low oxygen pressure. Arrows, ■, ⋀, # and * indicate the peak position for Co_3O_4, CoO, Fe_3O_4, MnO and $ZnMn_2O_4$ phases, respectively. The Mn and Fe patterns have been shifted upwards (2500 and 5000 counts, respectively) for the sake of clarity.

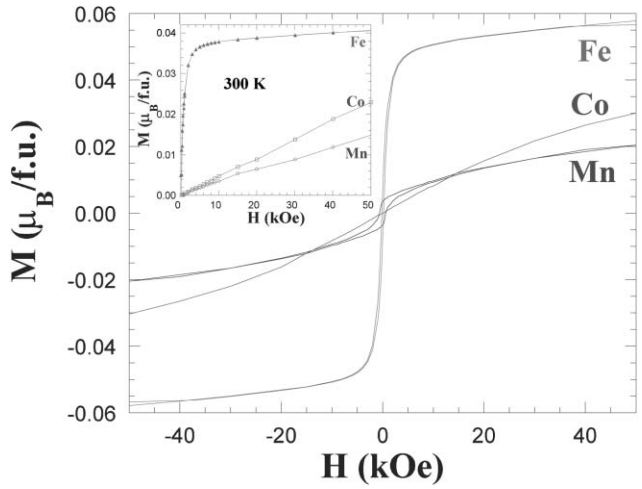

Fig. 5 Magnetization loops for Mn-, Fe- and Co-doped samples of Fig. 4 at 5 K. The data for the Mn and Co samples have been multiplied by five and four, respectively for the sake of comparison. Inset: isothermal magnetization at 300 K for the three samples. Here, the data of the Mn and Co samples have been multiplied by 30.

pressure. Similar refinements were obtained for the Fe compound. The refined lattice parameters for $Zn_{0.96}Mn_{0.04}O$ are a = 3.2567(2) and c = 5.2119(2) Å, revealing an expansion of the cell volume with respect to the undoped sample in agreement with previous results.[14]

The case of Fe compounds is more ambiguous. Some batches are single-phase while others show tiny amounts of FeO ($\sim$0.3%). In any case, the single phase can be obtained by an additional sintering step at 900 °C. Its lattice parameters show smaller differences with respect to ZnO. Then, the refined cell for $Zn_{0.96}Fe_{0.04}O$ is a = 3.2525(2) and c = 5.2025(2) Å, also very close to previous reports.[14] The Co-based sample instead showed minor amounts of CoO and metallic Co. This fact makes evident that Co oxides are easily reduced at this temperature in this low pO_2.

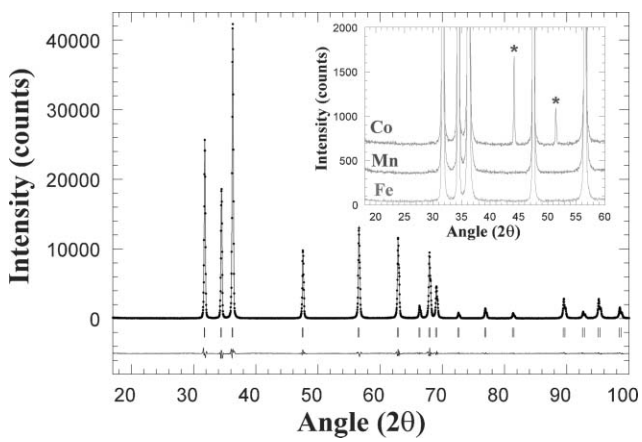

Fig. 6 The observed (points) and calculated (line) X-ray diffraction patterns for $Zn_{0.96}Mn_{0.04}O$ synthesized at 850 °C in a low oxygen pressure. The difference profile and reflection positions are also displayed at the bottom. Inset: detail of the X-ray patterns for Co-, Mn- and Fe-based samples in the same synthetic conditions. Asterisks stand for Co peaks.

The variation of the total pressure down to 2 bars does not change significantly the composition of the samples with the exception of the Co-based sample where only metallic Co is detected as secondary phase (there is no sign of CoO in the pattern). The inset of Fig. 6 shows the patterns collected for the samples prepared in these conditions.

The single phases, $Zn_{0.96}Mn_{0.04}O$ or $Zn_{0.96}Fe_{0.04}O$ are paramagnets down to 5 K whereas the Co-based sample shows a significant ferromagnetic contribution arising from the Co metal. For instance, Fig. 7 shows the magnetization curves at 5 K for the samples prepared at 850 °C in 2 bars of total pressure. Both single phases have hysteresis-free magnetization curves characteristic of the Langevin function for paramagnets. The loop for the Co sample instead is typical of a soft ferromagnet.

3.3. Samples prepared by ceramic procedure in inert atmosphere

Single phases of $Zn_{0.96}Mn_{0.04}O$ and $Zn_{0.96}Co_{0.04}O$ can be obtained by sintering in a current flow of Ar at 1150 °C. The Fe-based sample instead showed magnetite as secondary phase. $Zn_{0.96}Mn_{0.04}O$ can also be prepared at 925 °C but the Co-based sample showed traces of CoO suggesting an incomplete reaction. Nevertheless, it seems that single phases of $Zn_{0.96}Mn_{0.04}O$ and $Zn_{0.96}Co_{0.04}O$ can be achieved at lower temperatures using Ar atmosphere instead of air.[14] Structural refinements were performed on the patterns of both samples. The Mn compound showed similar results to those reported in section 3.2. The refinement for the single-phase $Zn_{0.96}Co_{0.04}O$ is displayed in Fig. 8. The refined lattice parameters for $Zn_{0.96}Co_{0.04}O$ are a =3.2512(2) and c =5.2027(2) Å, quite similar to the ones obtained for $Zn_{0.96}Fe_{0.04}O$ in section 3.2. This result can be understood in terms of the similar ionic sizes of high spin Fe^{2+} and Co^{2+}.[25]

The magnetic properties are in accordance with the compositions of the samples and only the Fe-based sample showed spontaneous magnetization up to room temperature

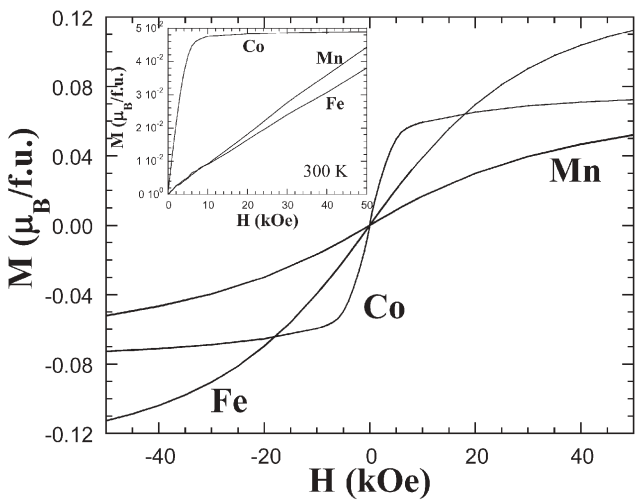

Fig. 7 Magnetization loops for Mn-, Fe- and Co-doped samples of Fig. 6 at 5 K. Inset: isothermal magnetization at 300 K for the three samples. The data of the Mn and Fe samples have been multiplied by 10 for the sake of comparison only in the inset.

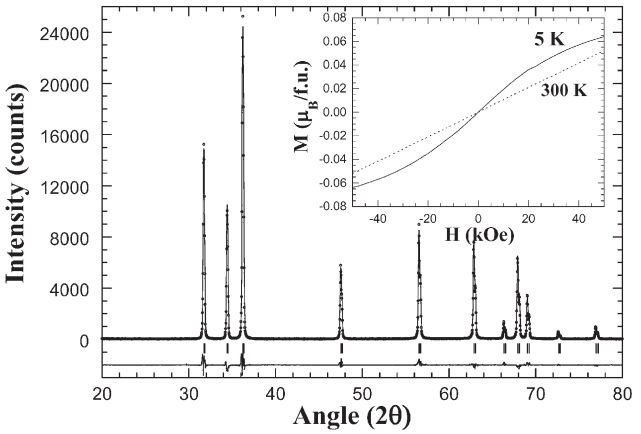

Fig. 8 Rietveld plots for $Zn_{0.96}Co_{0.04}O$ synthesized at 1150 °C in an Ar current flow. The symbols have the same meaning as in Fig. 6. Inset: magnetization loops at 5 K and at 300 K for this sample. The data at 300 K have been multiplied by 20 for the sake of comparison.

arising from the presence of magnetite. Both $Zn_{0.96}Mn_{0.04}O$ and $Zn_{0.96}Co_{0.04}O$ are paramagnets in the whole temperature range. For example, the anhysteretic loops for the latter compound at 5 and 300 K are shown in the inset of Fig. 8.

3.4. Samples obtained by sol–gel method

The precursor resin obtained from firing the gel was mainly non-crystalline and the X-ray diffraction patterns only showed very broad peaks arising from carbonaceous species. This resin was calcined in different conditions. Firing in an oxygen current flow at 400 °C for only 1 h gives a single phase for the Co-based sample but the Mn- and Fe-based samples showed secondary phases, namely $ZnMn_2O_4$ and Fe_3O_4, respectively. It is worth mentioning that this procedure is able to produce undoped ZnO with a high crystallinity in a very short time and very soft synthetic conditions.

The firing of the resin at 600 °C in a flow of Ar for 4 h only gives a single phase for the Mn-based sample. In the other two samples, the corresponding metallic particles, iron or cobalt, are segregated. This fact is likely to be due to the reduced conditions created by the firing of residual organic material in an inert atmosphere.

Finally, the best atmosphere to obtain single phases for all samples is air. We have fired the resins in air at 500 °C for 1 h and this process is enough to obtain $Zn_{1-x}M_xO$ solid solutions. They exhibit broad diffraction peaks typical of small grain sizes. The average size was calculated by using the Scherrer equation[26] and averaging the results achieved from several diffraction peaks. We obtained average grain sizes of 117 ± 17, 155 ± 22 and 298 ± 48 Å for Fe-, Mn- and Co-based samples, respectively.

In order to prepare samples with even smaller grain sizes, we have fired the resins at 375 °C for 1 h. Fig. 9 displays the X-ray patterns collected for these compounds evidencing the lack of secondary phases. These samples are composed of grains whose sizes are 82 ± 7, 125 ± 24 and 212 ± 18 Å for Fe-, Mn- and Co-based samples, respectively.

The magnetic properties for these single phases seem not to depend significantly on the crystalline degree. All of them are

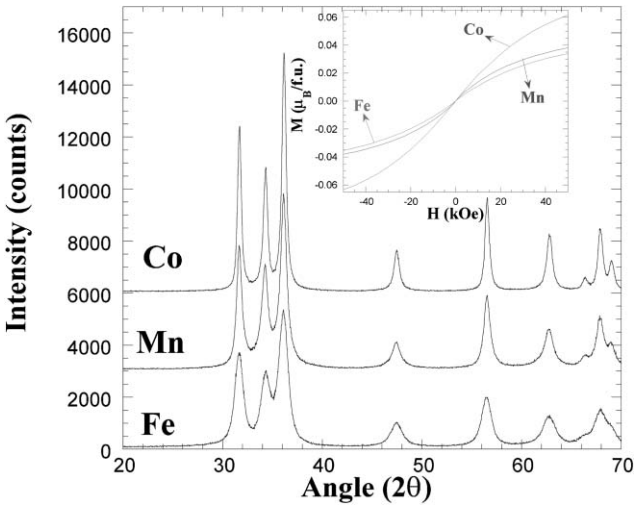

Fig. 9 Detail of the X-ray patterns for the Mn-, Fe- and Co-doped samples synthesized by firing a gel precursor at 375 °C in air for 1 h. Inset: magnetization loops at 5 K for the same samples obtained by firing the gel at 500 °C for 1 h.

paramagnetic in the whole temperature range, independent of the grain size. For instance, magnetization curves at 5 K are shown for the three compounds in the inset of Fig. 9. This result suggests the decrease of the grain size down to nanometric scale is not enough to develop ferromagnetism in this system and therefore, the ferromagnetic behavior observed in samples obtained by mechanical alloying is not clear at present.[13]

4. Discussion and conclusions

In this work we have checked different ways to prepare semiconductors oxides of ZnO doped with magnetic elements. The results together with the magnetic behavior are summarized in Table 1.

ZnO crystallizes in a hexagonal cell, space group $P6_3mc$, and the lattice parameters obtained in section 3.1 agree with the data reported in the literature.[14,27] The inclusion of Co^{2+} or Fe^{2+} leads to minor changes in the lattice. The *a* parameter slightly increases while the *c* parameter remains almost the same. This result indicates the incorporation of ionic species in the high spin state whose ionic radii are very similar to Zn^{2+}. Specifically, the ionic radii for four-fold coordination are 0.60, 0.58 and 0.63 Å for Zn^{2+}, high spin Co^{2+} and high spin Fe^{2+}, respectively.[25] The Mn compound instead shows a larger unit cell in agreement with the large high spin Mn^{2+} ion, ~0.66 Å.

Positively, bulk single phases are not magnetic independently of the grain size. This result is in agreement with refs. 14 and 15. The ferromagnetism of $Zn_{0.96}M_{0.04}O$ compounds arises from magnetic impurities whose composition depends on the synthetic conditions.

In Co-doped samples, the magnetic impurity corresponds to Co particles that can be formed in reducing conditions (low-oxygen pressure). This result is in agreement with the finding of Co particles in some $(Zn_{1-x}Co_x)O$ thin films and bulk materials.[9] Non-optimal synthetic conditions (oxidizing atmosphere or low temperature) lead to the formation of binary

Table 1 Summary of the main synthetic routes tested, phase composition and magnetic behaviour. PM and FM stand for paramagnetism and ferromagnetism

	Mn-based compound		Fe-based compound		Co-based compound	
Synthesis	Composition	Magnetism	Composition	Magnetism	Composition	Magnetism
Method a						
500 °C in air	ZnO + $ZnMnO_3$[a]	PM + FM (5–300 K)	ZnO + Fe_2O_3 + $Fe_{3-x}Zn_xO_4$	PM at 300 K, PM + FM at 5 K	ZnO + Co_3O_4	PM (5–300 K)
Method b						
a) 600 °C in Ar (175 or 2 bars)	ZnO + $ZnMn_2O_4$ + MnO	PM at 300 K, FM at 5 K	ZnO + Fe_3O_4	FM (5–300 K)	ZnO + Co_3O_4 + CoO	PM (5–300 K)
b) 850 °C in Ar (175 bars)	*$Zn_{0.96}Mn_{0.04}O$*	*PM (5–300 K)*	*$Zn_{0.96}Fe_{0.04}O$*[b]	*PM (5–300 K)*	ZnO + CoO + Co	FM (5–300 K)
c) 850 °C in Ar (2 bars)	*$Zn_{0.96}Mn_{0.04}O$*	*PM (5–300 K)*	*$Zn_{0.96}Fe_{0.04}O$*[b]	*PM (5–300 K)*	ZnO + Co	FM (5–300 K)
Method c						
a) 925 °C, Ar flow	*$Zn_{0.96}Mn_{0.04}O$*	*PM (5–300 K)*	ZnO + Fe_3O_4	FM (5–300 K)	$Zn_{0.96}Co_{0.04}O$ + CoO	PM (5–300 K)
b) 1150 °C, Ar flow	*$Zn_{0.96}Mn_{0.04}O$*	*PM (5–300 K)*	ZnO + Fe_3O_4	FM (5–300 K)	*$Zn_{0.96}Co_{0.04}O$*	*PM (5–300 K)*
Method d						
a) 400 °C, O_2 flow	ZnO + $ZnMn_2O_4$	PM at 300 K FM + PM at 5 K	ZnO + Fe_3O_4	FM (5–300 K)	*$Zn_{0.96}Co_{0.04}O$*	*PM (5–300 K)*
b) 600 °C, Ar flow	*$Zn_{0.96}Mn_{0.04}O$*	*PM (5–300 K)*	ZnO + Fe^0	FM (5–300 K)	ZnO + Co^0	FM (5–300 K)
c) 500 °C in air	*$Zn_{0.96}Mn_{0.04}O$*	*PM (5–300 K)*	*$Zn_{0.96}Fe_{0.04}O$*	*PM (5–300 K)*	*$Zn_{0.96}Co_{0.04}O$*	*PM (5–300 K)*
d) 375 °C in air	*$Zn_{0.96}Mn_{0.04}O$*	*PM (5–300 K)*	*$Zn_{0.96}Fe_{0.04}O$*	*PM (5–300 K)*	*$Zn_{0.96}Co_{0.04}O$*	*PM (5–300 K)*

[a] This phase actually corresponds to a spinel phase. [b] Traces of FeO appear in some batches. Single phases are written in italic characters

oxides (CoO or Co_3O_4) and the compounds exhibit paramagnetic behavior.

In Fe-doped samples, the magnetic impurity at room temperature could be either magnetite or metallic Fe. The latter phase needs strong reducing conditions to be segregated while the former can appear in samples sintered in air or inert atmosphere.

In Mn-doped compounds, we have only detected ferromagnetism at room temperature by using low sintering temperatures in agreement with previous results.[11,12,23] The rest of the preparations give rise to either non-magnetic single phases or magnetic impurities at low temperature (Mn_3O_4–$ZnMn_2O_4$). Therefore, the room-temperature ferromagnetism is very likely to be ascribed to secondary phases.[8,15] Recent microscopic findings reveal that Mn does not enter into the ZnO phase at 500 °C but Zn diffuses into the MnO_2 grains giving rise to spinel $Zn_xMn_{3-x}O_4$ phases.[23,28] The ferromagnetism is suggested to arise from the Zn diffusion front giving rise to a new surface magnetism.[28] We have also observed cubic spinels as secondary phase in our samples prepared at low temperature, see Fig. 1. This phase has also been observed by other researchers[20] and it has been ascribed to cubic $ZnMnO_3$.[14] The presence of Mn in an intermediate valence in the octahedral sites of these spinels could be argued as the ferromagnetic source. However, the presence of Zn^{2+} in the same octahedral sites is detrimental to establishing long range ordering. The detailed study of these new spinel phases will be subject of further surveys. Nevertheless, we can anticipate that none of these spinels are magnetic at room temperature. This is in agreement with the very small ferromagnetic component detected in the inset of Fig. 3. The exact identity of the magnetic impurity remains unclear so far.[8,28]

It is worth mentioning that our work makes it evident that the citrate sol–gel method provides an easy route to prepare doped transparent oxides with high homogeneity and small grain size. Using this procedure, we were successful in preparing single phases of doped ZnO with a very small grain size. The magnetic properties of these samples resemble those of the compounds prepared by standard ceramic procedures so the decrease of grain size cannot be the cause of the ferromagnetism reported for samples prepared by mechanical alloying.[13]

In conclusion, we were successful in preparing $Zn_{0.96}M_{0.04}O$ (M = Co, Fe and Mn) using different synthetic routes including very soft conditions. All of the single-phase samples behave as paramagnetic semiconductors without spontaneous magnetization in the whole temperature range. Ferromagnetism is only observed in samples exhibiting secondary phases. This feature indicates an extrinsic origin for the ferromagnetism observed in doped ZnO, casting doubts on its suitability for spintronics since it requires homogeneous materials whose magnetic properties do not arise from phase segregation.

Acknowledgements

Financial support from CICyT (projects MAT2005-04562 and MAT2005-02454) and DGA (PIP019/2005) are acknowledged. We also thank M. C. Sánchez and the Servicio Nacional EXAFS of Zaragoza University from technical support in the acquisition of X-ray patterns.

References

1 K. Sato and H. Katayama-Yoshida, *Jpn. J. Appl. Phys.*, 2001, **40**, L334; K. Sato and H. Katayama-Yoshida, *Physica B*, 2001, **308–310**, 904.
2 R. Janisch, P. Gopal and N. A. Spaldin, *J. Phys.: Condens. Matter*, 2005, **17**, R657.
3 C. Liu, F. Yun and H. Morkoc, *J. Mater. Sci. Mater. Electron.*, 2005, **16**, 555.

4 M. Venkatesan, C. B. Ftizgerald, J. G. Lunney and J. M. D. Coey, *Phys. Rev. Lett.*, 2004, **93**, 177206.
5 D. S. Kim, S. Lee, C. Min, H. M. Kim, S. U. Yuldashev, T. W. Kang, D. Y. Kim and T. W. Kim, *Jpn. J. Appl. Phys.*, 2003, **42**, 7217.
6 J. M. D. Coey, M. Venkatesan and C. B. Fitzgerald, *Nat. Mater.*, 2005, **4**, 173.
7 D. B. Buchholz, R. P. H. Chang, J. H. Song and J. B. Ketterson, *Appl. Phys. Lett.*, 2005, **87**, 082504.
8 D. C. Kundaliya, S. B. Ogale, S. E. Lofland, S. Dhars, C. J. Metting, S. R. Shinde, Z. Ma, B. Varughese, K. V. Ramanujachary, L. Salamanca-Riba and T. Venkatesan, *Nat. Mater.*, 2004, **3**, 709.
9 J. H. Kim, H. Kim, D. Kim, Y. Ihm and W. R. Choo, *J. Eur. Ceram. Soc.*, 2004, **24**, 1847; S. Deka and P. A. Joy, *Chem. Mater.*, 2005, **17**, 6507.
10 A. C. Mofor, A. El-Shaer, A. Bakin, A. Waag, H. Ahlers, U. Siegner, S. Sievers, M. Albrecht, W. Schoch, N. Izyumskaya, V. Avrutin, S. Sorokin, S. Ivanov and J. Stoimenos, *Appl. Phys. Lett.*, 2005, **87**, 062501.
11 P. Sharma, A. Gupta, K. V. Rao, F. J. Owens, R. Sharma, R. Ahuja, J. M. O. Guillen, B. Johansson and G. A. Gehring, *Nat. Mater.*, 2004, **2**, 673.
12 P. Sharma, A. Gupta, F. J. Owens, A. Inoue and K. V. Rao, *J. Magn. Magn. Mater.*, 2004, **282**, 115; O. D. Jayakumar, I. K. Gopalakrishnan and S. K. Kulshreshtha, *J. Mater. Chem.*, 2005, **15**, 3514.
13 H. J. Blythe, R. M. Ibrahim, G. A. Gehring, J. R. Neal and A. M. Fox, *J. Magn. Magn. Mater.*, 2004, **283**, 117.
14 S. Kolesnik, B. Dabrowski and J. Mais, *J. Appl. Phys.*, 2004, **95**, 2582.
15 S. Kolesnik and B. Dabrowski, *J. Appl. Phys.*, 2004, **96**, 5379; G. Lawes, A. S. Risbud, A. P. Ramirez and R. Seshadi, *Phys. Rev. B*, 2005, **71**, 045201; C. N. R. Rao and F. L. Deepak, *J. Mater. Chem.*, 2005, **15**, 573.
16 T. Dietl, H. Ohno, F. Matsukura, J. Cibert and D. Ferrand, *Science*, 2000, **287**, 1019.
17 J. Rodríguez-Carvajal, *Physica B*, 1992, **192**, 55, available at www-llb.cea.fr.
18 A. Guethert, R. Muenze and B. Eichler, *J. Radioanal. Chem.*, 1981, **62**, 91.
19 H. Toussaint, *Rev. Chim. Miner.*, 1964, **1**, 141.
20 S. Kolesnik, B. Dabrowski and J. Mais, *J. Supercond.*, 2002, **15**, 251.
21 B. L. Chamberland, A. W. Sleight and J. F. Weiher, *J. Solid State Chem.*, 1970, **1**, 512.
22 W. L. Roth, *J. Phys. Chem. Solids*, 1964, **25**, 1.
23 J. L. Costa-Krämer, F. Briones, J. F. Fernández, A. C. Caballero, M. Villegas, M. Díaz, M. A. García and A. Hernando, *Nanotechnology*, 2005, **16**, 214.
24 S. Asbrink, A. Warskowska, L. Gerward, J. S. Olsen and E. Talik, *Phys. Rev. B*, 1999, **60**, 12651.
25 R. D. Shannon, *Acta Crystallogr., Sect. A*, 1976, **32**, 751.
26 A. R. West, *Solid state chemistry and its applications*, John Wiley & Sons, Chichester, 1985, p. 173.
27 H. Sawada, R. Wang and A. W. Sleight, *J. Solid State Chem.*, 1996, **112**, 148.
28 M. A. García, M. L. Ruiz-González, A. Quesada, J. L. Costa-Kramer, J. F. Fernández, S. J. Khatib, A. Wennberq, A. C. Caballero, M. S. Martín-González, M. Villegas, F. Briones, J. M. González-Calbet and A. Hernando, *Phys. Rev. Lett.*, 2005, **94**, 217206.

